An Uncleavable Procaspase-3 Mutant Has a Lower Catalytic Efficiency but an Active Site Similar to That of Mature Caspase-3[†]

Kakoli Bose[‡], **Cristina Pop**[‡], **Brett Feeney**, and **A. Clay Clark**[*]
Department of Molecular and Structural Biochemistry, North Carolina State University, Raleigh, North Carolina 27695

Abstract

We have examined the enzymatic activity of an uncleavable procaspase-3 mutant (D9A/D28A/D175A), which contains the wild-type catalytic residues in the active site. The results are compared to those for the mature caspase-3. Although at pH 7.5 and 25 °C the K_m values are similar, the catalytic efficiency (k_{cat}) is ~130-fold lower in the zymogen. The mature caspase-3 demonstrates a maximum activity at pH 7.4, whereas the maximum activity of procaspase-3 occurs at pH 8.3. The pK_a values of both catalytic groups, H121 and C163, are shifted to higher pH for procaspase-3. We developed limited proteolysis assays using trypsin and V8 proteases, and we show that these assays allow the examination of amino acids in three of five active site loops. In addition, we examined the fluorescence emission of the two tryptophanyl residues in the active site over the pH range of 2.5–9 as well as the response to several quenching agents. Overall, the data suggest that the major conformational change that occurs upon maturation results in formation of the loop bundle among loops L4, L2, and L2′. The pK_a values of both catalytic groups decrease as a result of the loop movements. However, loop L3, which comprises the bulk of the substrate binding pocket, does not appear to be unraveled and solvent-exposed, even at lower pH.

Caspase-3 is a cysteinyl aspartate-specific protease that is known as the executioner protease in apoptosis. During apoptosis, a number of key structural proteins, cell cycle control proteins, and DNase inhibitors are cleaved (1), resulting in an organized dismantling of the cell. These reactions play central roles in development and homeostasis in eumetazoans (2), while altered regulation of apoptosis leads to a variety of diseases (3). The caspase protease family can be divided into three subgroups (4, 5), the activator caspases, the executioner caspases, and those involved in the inflammatory response. Caspases in two of the subgroups (activators and executioners) are involved in apoptosis.

In contrast to the activator caspases, procaspase-3 is a dimer *in vitro* (6, 7) and *in vivo* (8). Although there is a large pool of procaspase-3 in the cell (~100 nM) (9), it is unclear why the protein is inactive. The structures of several mature caspases, with inhibitors bound, have been determined (10–16), but until recently, structural information of the procaspases was not available. The procaspase primary structure is organized as an N-terminal pro

[*]To whom correspondence should be addressed: Department of Molecular and Structural Biochemistry, 128 Polk Hall, North Carolina State University, Raleigh, NC 27695-7622. Phone: (919) 515-5805. Fax: (919) 515-2047. clay_clark@ncsu.edu.
[‡]These authors contributed equally to this work.

domain, which varies in size in the three subgroups, a large subunit of ~180 amino acids, a short (~20 amino acids) intersubunit linker, and a small subunit of ~100 amino acids. In general, caspases are activated in a two-step process in which the protein is cleaved at an aspartate residue in the intersubunit linker followed by one or more cleavages that remove the pro domain (17). In the case of procaspase-3, cleavage at D175, in the intersubunit linker, is sufficient to allow for full activity (18). The protein is cleaved then at D9 and D28 so that the pro domain is removed.

The structure of procaspase-7, described by Chai *et al.* (19) and Riedl *et al.* (20), has allowed a detailed comparison of the caspase structure as it undergoes maturation (21) (see Figure 1). Procaspase-7 is thought to represent the executioner subgroup of caspases, and indeed, the amino acid sequences of caspases-3 and -7 are 55% identical. The structures of mature caspase-3 and of procaspase-7 are summarized in Figure 1 and show that the two proteins are very similar. The differences between the two forms of the proteins are observed primarily in four surface loops (L1–L4) that comprise the active sites. Current models (19, 20) hypothesize that formation of the substrate binding pocket in caspases is a multistep process following cleavage of the L2–L2′ loop in the proenzyme. First, release of the L2 and L2′ segments allows conformational changes in other loops that must occur before induced fit remodels the active site around the substrate. Recent reports of low activity in the zymogen (22) are inconsistent with this model, as the cleavage is an absolute prerequisite for forming the active site. Nicholson and co-workers used an active site probe that required catalytic turnover to covalently modify the active site cysteine to show that procaspase-3 is catalytically competent (22). That procaspase-3 has enzymatic activity is in keeping with results for other procaspases (procaspases-1, -8, and -9, for example) (23–25), which clearly show that the procaspases contain enzymatic activity when the pro forms are recruited into the oligomeric scaffolds.

To further examine this issue, we studied the enzymatic activity of an uncleavable procaspase-3 mutant (D9A/D28A/D175A) in which the three processing sites were removed. While this mutant cannot be processed, it contains the wild-type catalytic residues in the active site. We show that the proenzyme activity demonstrated previously (22) is due to a decrease in k_{cat} rather than K_m relative to that of the mature enzyme. This means that maturation is not required for substrate binding. We developed several assays, including protease sensitivity, intrinsic fluorescence, and fluorescence emission quenching, to examine the conformational changes in procaspase-3 that occur as a result of maturation. Overall, the results show that the active site conformations of these two forms of the protein are similar, although not identical. In particular, the residues in loop L3 do not behave as one would expect for an unraveled flexible loop. The observations described here, as well as those presented in the accompanying paper (46), will require some changes in the details of the activation model for procaspase-3.

MATERIALS AND METHODS

Materials

Bovine serum albumin, CHAPS, DTT, TLCK, monobasic and dibasic potassium phosphate, Trizma base, citric acid, sodium citrate (dihydrate), sodium bicarbonate, PIPES, potassium iodide, acrylamide, and diisopropyl fluorophosphate (DFP) were from Sigma. Sodium chloride and glycine were from Fisher. Sucrose was from Mallinckrodt. Acetonitrile and HEPES were from Acros. α-Cyano-4-hydroxycinnamic acid and sinapinic acid were from Aldrich. V8 protease and trypsin were from Roche Biochemicals. Cesium chloride was from Harshaw. Ultrapure urea was purchased from Nacalai Tesque Inc. (Kyoto, Japan). Ac-DEVD-AFC, Ac-DEVD-CHO, and Z-VAD-FMK were purchased from Calbiochem. His-bind resin was from Novagen.

Plasmid Construction

Procaspase-3 mutants were created using the Quick-Change site-directed mutagenesis kit (Strat-agene) and the primers described below. The procaspase-3(D9A/D28A/D175A) mutant was made by a three-step process from plasmid pHC332 (6), harboring the gene for wild-type human procaspase-3. First, D175 was mutated to alanine using primer 1 (5′-GTGGCATTGAGACAG**CT**AGCGGTGTTGATGATG-3′) and primer 2 (5′-CATCATCAACACC**GCTAGC**TGTCTCAATGCCAC-3′). In the background of D175A, D28 was mutated to alanine using primer 3 (5′-GGAAGCGAATCAA**TGGCCAG**TGGAATATCCCTG-3′) and primer 4 (5′-CAGGGATATTCCA**CTGGCC**ATTGATTCGCTTCC-3′). In the background of D28A/D175A, D9 was mutated to alanine using primer 5 (5′-GAAAACTCAGTGG**CTAGC**AAATCCATTAAAAATTTGG-3′) and primer 6 (5′-CCAAATTTTTAATGGATTT**GCTAG**CCACTGAGTTTTC-3′). The primers incorporated the following restriction sites for screening mutants: *Nhe*I for primers 1 and 2, *Bal*I (*Msc*I) for primers 3 and 4, and *Nhe*I for primers 5 and 6. The mutations are shown in bold, and the restriction sites are underlined. All plasmids were sequenced (both strands) to confirm the mutations. The resulting plasmid is called pHC33209, and we refer to this mutant as procaspase-3(D$_3$A).[1] The plasmids for procaspase-3(C163A/W206Y) and procaspase-3(C163A/W214V) were kindly provided by G. Salvesen (Burnham Institute).

Protein Purification

All proteins were purified as described previously (6), with the following modifications. Cells were grown in LB medium at 37 °C. After induction with 0.4 mM IPTG at an A_{600} of ~1.2, the temperature was lowered to 25 °C. The cells were harvested after induction for 4 h [procaspase-3(D$_3$A) and caspase-3] or 18 h (all other proteins). Following lysis, the supernatant was separated from cell debris by centrifugation at 28000g (SA-600 rotor) for 30 min at 4 °C. The supernatant was batch-bound for 30 min to His-bind resin (15 mL) that had been pre-equilibrated in buffer A [50 mM Tris-HCl (pH 7.9), 50 mM NaCl, 5 mM imidazole, 50 μg/mL TLCK, 50 μg/mL TPCK, and 100 μg/mL PMSF]. The resin was washed four times with 4 volumes of buffer A, and then four times with 4 volumes of buffer A containing 80 mM imidazole. After each wash, the resin was centrifuged for 2 min at 500g (SA-600 rotor), and the supernatant was removed. The protein was eluted with buffer A (two times with 2 volumes each) containing 500 mM imidazole, and the fractions were analyzed by SDS–PAGE. The proteins were further purified by DEAE-Sepharose chromatography as described previously (6). The concentrations of the proteins were determined as described by Edelhoch (26), and the protein concentrations reported here are those of the monomer.

Enzyme Activity Assay

The activities of mature caspase-3 and of procaspase-3(D$_3$A) were determined as described previously (27) using the fluorescent substrate Ac-DEVD-AFC. Assays were performed in a buffer containing 20 mM Pipes, 100 mM NaCl, 0.1% CHAPS, 10% sucrose, and 10 mM DTT, at 25 °C (enzyme assay buffer). The total reaction volume was 200 μL, and the final concentration of the enzymes was either 1 nM (caspase-3) or 10 nM [procaspase-3(D$_3$A)]. Samples were excited at 400 nm, and the fluorescence emission was monitored at 505 nm. All fluorescence measurements were acquired using a PTI C-61 spectrofluorometer (Photon Technology International). The instrument was equipped with a thermostated cell holder, and the temperature was held constant at 25 °C using a circulating water bath. The steady-

---

[1]Abbreviation: procaspase-3(D$_3$A), procaspase-3(D9A/D28A/D175A).

state parameters, K_m and k_{cat}, were determined from plots of initial velocity versus substrate concentration.

The initial velocity was determined over the pH range of 5–10 as described previously (28). The following buffers were used: 50 mM citrate (pH 3.0–6.2), 20 mM Pipes (pH 6.1–7.5), 50 mM Tris-HCl (pH 7.2–9.0), 50 mM bicine (pH 7.6–9.0), 100 mM glycine (pH 8.6–10.6), and 50 mM sodium bicarbonate (pH 9.2–10.6). All buffers contained 100 mM NaCl, 0.1% CHAPS, 1% sucrose, and 10 mM DTT. Final protein concentrations were 2.5 nM (caspase-3) or 25 nM [procaspase-3(D$_3$A)]. The data (initial velocity vs pH) were fit to eq 1:

$$\log Y = C(1 + [H^+]/K_{a1} + K_{a2}/[H^+]) \tag{1}$$

where Y is the initial velocity measured at each pH, C is the pH-independent value of Y, and K_{a1} and K_{a2} are the dissociation constants for the enzyme groups (29).

Immunoblots

Polyclonal anti-caspase-3 antibody (#9662) was from Cell Signaling Technology. Alkaline phosphatase-coupled secondary antibody (goat anti-rabbit), BCIP (5-bromo-4-chloro-3-indoyl phosphate *p*-toluidine salt) and NTB (*p*-nitro blue tetrazolium chloride) were from Bio-Rad. All steps were performed at room temperature unless otherwise noted. Proteins, in amounts indicated in the figure legends, were subjected to SDS–PAGE (10 to 25% gradient). The proteins from the gel were transferred to a PVDF membrane as described previously (30), and the membrane was washed once for 5 min with TBS-T solution [15 mL of 20 mM Tris-HCl (pH 7.6), 0.15 M NaCl, and 0.1% Tween-20]. The membrane was then blocked by adding blocking buffer [15 mL of TBS-T containing 5% nonfat dry milk (Bio-Rad)] for 1 h. The membrane was washed three times with TBS-T (20 mL) for 5 min each, and the membrane was then incubated with primary antibody (10 mL of a 1:1000 dilution in blocking buffer) overnight at 4 °C. The membrane was washed with TBS-T as described above and then incubated with secondary antibody (20 mL of a 1:3000 dilution in blocking buffer) for 1 h. Excess secondary antibody was removed by washing the membrane with TBS-T as described above. The colorimetric reaction was performed according to the manufacturer's instructions.

Digestion of Procaspase-3 with Mature Caspase-3

Procaspase-3(C163S) or procaspase-3(D$_3$A) was diluted into enzyme assay buffer so that the final volume was 100 μL, and the final concentration of procaspase was 5 μM. Caspase-3 was added at a caspase:procaspase molar ratio of 1:20, and the mixture was incubated at 25 °C. At the times indicated in the figure, aliquots (20 μL) were removed, and the caspase was inhibited with Z-VAD-FMK (1 μL of a 20 mM stock). The samples were analyzed by SDS–PAGE (10 to 25% gradient) and stained with Coomassie blue.

Limited Proteolysis with Trypsin

Proteins (all 15 μM) were digested with 1/15 of their concentration (w/w) of trypsin in a buffer of 20 mM Tris-HCl (pH 7.2) and 0.5 mM DTT at 25 °C. After trypsin was added, aliquots were withdrawn at prescribed time intervals, and reactions were inhibited by TLCK [thrice the concentration of trypsin (w/w)]. The samples were frozen at −20 °C until they were analyzed. Samples were analyzed by SDS–PAGE using either 4 to 25% or 10 to 25% polyacrylamide gradient gels. In separate experiments, the caspase-3 inhibitor, Ac-DEVD-CHO (thrice the concentration of the protein), was included. Protein fragment identification was done by MALDI-TOF mass spectrometry and peptide sequencing as described below.

Limited Proteolysis with V8 Protease

Proteins (all 15 μM) were digested with 1/15 of their concentration (w/w) of V8 protease in a buffer of 20 mM Tris-HCl and 0.5 mM DTT (for experiments at pH 7.8 and 7.2) or a buffer of 10 mM citrate and 0.5 mM DTT (for experiments at pH 6.0, 5.0, and 4.0), at 25 °C. After the addition of protease, aliquots were withdrawn at prescribed time intervals, and the reactions were inhibited with DFP [thrice the concentration of V8 (w/w)]. Samples were frozen at −20 °C until they were analyzed. Samples were analyzed by SDS–PAGE using either 4 to 25% or 10 to 25% polyacrylamide gradient gels. In separate experiments, the caspase-3 inhibitor Z-VAD-FMK (thrice the concentration of the protein) was included. Protein fragment identification was done by MALDI-TOF mass spectrometry and peptide sequencing, as described below.

Kinetic analysis of the fragments was carried out by using the ImageQuant software (Molecular Dynamics). The fraction of species relative to the full-length protein at time zero was plotted, and the data were fit to a double-exponential equation for bands 1–4 and to a single-exponential equation for 16, 8, and 4 kDa bands.

MALDI-TOF Mass Spectrometry

Experiments were performed with a Bruker Proflex III instrument that is equipped with a nitrogen laser (λ = 337 nm, 3 ns pulse width), deflection capabilities, delayed extraction, and an extended flight tube. The mass accuracy for analyte molecules is ±0.1% with external calibration. Matrices used for these experiments were saturated solutions of sinapinic acid (α-cyanohydroxycinnamic acid) or α-cyano-4-hydroxycinnamic acid in acetonitrile, water, and TFA [50:50:0.1 (v/v)]. Calibration was done with ubiquitin (8 kDa), myoglobin (17 kDa), and bovine serum albumin (66.5 kDa). Samples from the limited proteolysis experiments were crystallized on a target plate with a matrix solution (1:1). Desalting of the peptides was done with Ziptip pipet tips (Millipore). Experiments were performed at 22–26 attenuation and 50 shots. Each experiment was repeated at least five times, and the averaged data were collected.

Peptide Sequencing

The gels for trypsin and V8 protease digestions were transferred to a PVDF membrane as described previously (30), and the first five amino-terminal amino acids were determined by Edman degradation (Protein Structure Core Facility, University of Nebraska, Lincoln, NE).

Quenching of Tryptophan Fluorescence Emission

Stock protein solutions were dialyzed against a buffer of 50 mM potassium phosphate (pH 7.2) and 1 mM DTT. Alternatively, the proteins were dialyzed against a buffer of 20 mM citrate and 1 mM DTT (pH 6.0–3.0). Stock solutions of acrylamide, KI, or CsCl (quenchers) were prepared in the same buffers. Protein solutions (1 μM) were prepared from the stocks, and the quenching agent was added to the final concentrations shown in the figures. The samples were stirred and incubated for 5 min following each addition of quencher, and the experiments were performed at 25 °C. Samples were excited at 295 nm, and the fluorescence emission was examined from 300 to 400 nm. All data were corrected for the background signal. For pH-dependent quenching studies, the following buffers were used: 50 mM sodium citrate (pH 3–6.5), 50 mM potassium phosphate (pH 6.0–8.0), or 50 mM Tris-HCl (pH 7.2–9.5). All buffers contained 1 mM DTT.

Data Analysis

For acrylamide and CsCl quenching, the data were fit to the Stern–Volmer equation, accounting for static and dynamic quenching (31). For quenching by iodide, the percent

quenching [$(\Delta F/F_0) \times 100$] was plotted versus the concentration of KI, and the data were fit to eq 2:

$$(\Delta F/F_0) \times 100 = (100 K_{SV}[Q]f_a)/(1+K_{SV}[Q]) \tag{2}$$

where ΔF is the change in fluorescence emission at each concentration of quencher (KI), F_0 is the fluorescence intensity of the protein in the absence of the quencher, K_{SV} is the Stern–Volmer constant, [Q] is the quencher concentration, and f_a is the fraction of the initial fluorescence emission that is accessible to the quencher.

The Stern–Volmer constants (K_{SV}), determined from the fits described by eq 2, over the pH range of 2.5–9, were plotted versus pH. The data were fit to eq 3:

$$K_{SV} = A + \Delta K_{SV_1} \times 10^{n_1(\text{pH}-pK_{a1})}/[1+10^{n_1(\text{pH}-pK_{a1})}] + \Delta K_{SV_2} \times 10^{n_2(\text{pH}-pK_{a2})}/[1+10^{n_2(\text{pH}-pK_{a2})}] \tag{3}$$

where K_{SV} is the Stern–Volmer constant, A is the value of K_{SV} at the lowest pH, ΔKSV_1 and ΔKSV_2 represent the changes in the Stern–Volmer constant for each transition, n_1 and n_2 are cooperativity parameters for each transition, and pK_{a1} and pK_{a2} are the apparent pK values of the transitions.

Fluorescence Emission Versus pH

Proteins were dialyzed against a buffer of 20 mM citrate at pH 6.0 (for experiments between pH 2.5 and 6.2) or a buffer of 20 mM phosphate at pH 9.0 (for experiments between pH 6.0 and 9.0). Dialysis buffers contained 1 mM DTT. Protein solutions (1 μM) ranging from pH 2.5 to 9.0 were prepared and incubated in a water bath at 25 °C for at least 1 h. Samples were excited at 280 nm, and the fluorescence emission was monitored between 305 and 400 nm. All measurements were corrected for the background signal. For each solution, the average emission wavelength was determined as described previously (32) using eq 4

$$\langle\lambda\rangle = \sum_{i=1}^{N} I_i\lambda_i / \sum_{i=1}^{N} I_i \tag{4}$$

where $\langle\lambda\rangle$ is the average emission wavelength and I_i is the fluorescence emission at wavelength λ_i. Plots of $\langle\lambda\rangle$ versus pH were fit to eq 5 (33):

$$\langle\lambda\rangle = A + \Delta\langle\lambda\rangle_{(1)} \times 10^{n_1(\text{pH}-pK_{a1})}/[1+10^{n_1(\text{pH}-pK_{a1})}] + \Delta\langle\lambda\rangle_{(2)} \times 10^{n_2(\text{pH}-pK_{a2})}/[1+10^{n_2(\text{pH}-pK_{a2})}] \tag{5}$$

where A is the value of $\langle\lambda\rangle$ at pH >8.0, $\Delta\langle\lambda\rangle_{(1)}$ is the change in $\langle\lambda\rangle$ for the first transition, $\Delta\langle\lambda\rangle_{(2)}$ is the change in $\langle\lambda\rangle$ for the second transition, n_1 and n_2 are cooperativity parameters for transitions 1 and 2, respectively, and pK_{a1} and pK_{a2} refer to the apparent pK values of the first and second transitions, respectively.

RESULTS

Enzymatic Activity of Procaspase-3(D$_3$A)

Nicholson and co-workers (22) demonstrated that procaspase-3 is catalytically competent by using an active site probe that required catalytic turnover to covalently modify the active site

cysteinyl residue. While the catalytic parameters were not described, they concluded that procaspase-3 contains sufficient activity to carry out autolytic cleavage. To examine the catalytic parameters of procaspase-3, we generated a mutant in which the three aspartate residues that are cleaved during processing were mutated to alanine (D9A/D28A/D175A). This mutant, called procaspase-3(D$_3$A), is comparable to the D9E/D28E/D175E triple mutant and the D28A/D175A double mutant described by Nicholson and coworkers (22), who showed that the mutations prevented autoprocessing. The active site catalytic residues (C163 and H121) were kept intact, thus generating an uncleavable procaspase-3 with the active site cysteine unchanged. We used the Asp to Ala triple mutant rather than the Asp to Glu mutants to ensure that the procaspase does not autoprocess. Stennicke *et al*. (34) showed that while the Asp/Glu selectivity ratio at P1 is ~20000, there was no measurable hydrolysis with Ala at P1. In addition, the three residues are in flexible regions of the protein, which are not observed in the crystal structures, so we hypothesize that the mutations are not structurally perturbing.

For procaspase-3(D$_3$A), the initial velocity was measured over a range of substrate concentrations, and the results are compared to those of mature caspase-3 (Figure 2A). The data demonstrate that procaspase-3(D$_3$A) binds the tetrapeptide substrate and is catalytically active, although the activity is much lower than that of the mature caspase-3. The steady state parameters, K_m and k_{cat}, determined from the data in Figure 2A, are presented in Table 1. The results show that the values of K_m are comparable in the two proteins, between ~2 and 4 μM. For caspase-3, these parameters are similar to those published previously (34, 35). As shown in Table 1, the catalytic efficiency, k_{cat}, for procaspase-3(D$_3$A) is ~130-fold lower than that of the mature caspase-3. Overall, the specificity constant (k_{cat}/K_m) is ~200-fold lower in the procaspase than in the mature caspase-3. It has been shown that both active sites in the caspase-3 heterotetramer are catalytically active (27). We find that this is also true for procaspase-3(D$_3$A) (data not shown).

We examined the pH dependence of the enzyme activity, and the results are shown in Figure 2B. For mature caspase-3, the results are in good agreement with those described previously (28) and demonstrate a bell-shaped profile. The results are consistent with the protonation and/or deprotonation of the two catalytic groups, C163 and H121, leading to one active form of the enzyme with a maximum activity between pH 7.2 and 7.8. The apparent pK_a values of the two transitions are 6.3 and 8.5, respectively, again, in good agreement with previous results (28). Procaspase-3(D$_3$A) also exhibits a bell-shaped pH profile (Figure 2B), although when compared to that of the mature caspase-3, the profile is shifted to higher pH so that the maximum activity occurs between pH 8.0 and 8.5. The apparent pK_a values of the two transitions are 7.3 and 9.1, respectively.

The increase in activity is thought to be due to the deprotonation of the cysteine (36) so that the doubly ionized form, S$^-$Im$^+$, is the active form of the protein. The data presented here show that the environments of both groups change upon maturation, resulting in a decrease in the pK_a values of both groups.

Characterization of Procaspase-3(D$_3$A)

Formally, it is possible that minor cleavage reactions occur at sites in the intersubunit linker other than D175. While to our knowledge there is no evidence of support in the literature, it is possible that the protein is cleaved at TELD169 or SGVD179. This seems to be unlikely for the following reasons. First, using an anti-caspase-3 antibody raised against the large subunit of human caspase-3, Nicholson and co-workers showed that there was no autocatalytic processing of procaspase-3(D28A/D175A) when the protein was expressed in *Escherichia coli* (22). Thus, while the protein is active, no processed large subunit was observed. Second, Salvesen and co-workers showed that uncleavable procaspase-9 mutants

(D315A and/or D330A) contained small amounts of protein processed at an alternate site in the intersubunit linker (25); however, it was shown that the unprocessed D315A/D330A mutant is responsible for the observed activity, not the alternatively cleaved caspase.

Several experiments were carried out in an effort to examine the possibility that the enzymatic activity described in the legend of Figure 2 for procaspase-3(D_3A) was due to a small amount of contaminating mature caspase-3. First, we examined the procaspase-3(D_3A) using an antibody to the large subunit, and the results are shown in Figure 3A. The data show no evidence of the processed large subunit in the sample. From dilution experiments of the mature caspase-3 (Figure 3A), we estimate that the detection limit is 1:500 or greater. This suggests that if a small amount of contaminating mature caspase-3 were present in the sample of procaspase-3(D_3A) at concentrations 1/200 of that of the procaspase, then we would detect it in this assay. The ratio of 1:200 would be consistent with the observed difference in enzyme activities (Table 1). Second, we examined the cleavage of procaspase-3(C163S) and of procaspase-3(D_3A) by mature caspase-3, and the results are shown in Figure 3B. As described previously (6), procaspase-3(C163S) is a catalytically inactive variant of the procaspase. The procaspases were incubated with mature caspase-3 for up to 16 h, and aliquots were examined by SDS–PAGE. The data show that procaspase-3(C163S), which is inactive yet contains the three processing sites, is cleaved by caspase-3 at D9, D28, and D175, giving rise to five protein fragments, labeled bands 2–7 in Figure 3B. Bands 2 and 3 represent cleavage of the procaspase at D9 and D28, respectively, resulting in removal of the propeptide. Bands 4 and 5 represent cleavage at D175, to separate the two subunits, but the large subunit contains all or part of the propeptide. Bands 6 and 7 represent the processed large (17 kDa) and small (12 kDa) subunits, respectively. In contrast, procaspase-3(D_3A) was not cleaved by the mature caspase-3 (Figure 3B) even after incubation overnight. These results demonstrate that removal of the three processing sites prevents processing of the procaspase by the active caspase-3.

If the enzyme activity of the procaspase-3(D_3A) were due to a small amount of contaminating mature caspase, then it is possible that this would be reflected in the steady-state parameters determined for the procaspase (Table 1). That is, one might observe that the K_m was the same as that of the mature caspase, but the k_{cat} was much lower. One could then argue that the lower k_{cat} was due to the low concentration of the contaminant. However, we note that one would not expect the pH profile of the enzyme activity to change if the activity were due simply to a 1:200 concentration of contaminating active caspase-3. One would expect to observe the same pH profile shown in Figure 2 above. We show this in Figure 3C. The mature caspase-3 was diluted to the concentration expected for a 1:200 contaminant of the procaspase, and the enzyme activity was measured versus pH. While there is more scatter due to the low protein concentration, we observe that the pH profile agrees well with that shown in Figure 2B for the mature caspase-3. The maximum activity is observed in the range of pH 7.2–7.8, and the pK_a values of the active site groups are 6.6 and 8.5, in good agreement with those of the mature caspase-3 shown above (Figure 2B and Table 1). In addition, we added mature caspase-3 (50 pM) to the sample of procaspase-3(D_3A) (10 nM) to simulate a 1:200 concentration of contaminant. The results of the enzyme assays of the mixture are shown in Figure 3D. The data do not produce a simple bell-shaped profile but rather appear to reflect the enzyme activity of both enzymes. For example, the data demonstrate a maximum at pH ~7.5 and an inflection at pH ~8.5. The results are in good agreement with the maximal activities observed for the two individual proteins (Table 1). The data in Figure 2B for the individual proteins were scaled and added, and the results are shown in Figure 3D. The results indicate that the experimental data for the mixture represent the sum of the two individual enzyme activities.

On the basis of the results of the experiments shown in Figures 2 and 3, we suggest that the enzyme activity measured for the procaspase-3(D_3A) is not due to a contaminating mature caspase but rather reflects the intrinsic properties of the procaspase.

Limited Trypsin Proteolysis

We examined the conformation of procaspase-3 and of caspase-3 by limited trypsin proteolysis. A time course analysis of the procaspase-3(C163S) digestion with trypsin showed several discrete cleavages (Figure 4A). We note that in these assays there was no difference between the results obtained for procaspase-3(C163S) and procaspase-3(D_3A) (not shown). Thus, in these assays, we consider the two procaspase variants to be equivalent. Also, minor contaminants of ~24 and ~15 kDa were observed in the stock protein (time zero in Figures 4A and 5A) for procaspase-3(C163S). There was no reaction of these bands with a caspase-3 antibody raised against the large subunit (described in the legend of Figure 3A), demonstrating that the proteins were from *E. coli* rather than processed procaspase-3(C163S).

We analyzed the digests by MALDI-TOF mass spectrometry (not shown), and the results showed protein fragments of 25, 16, 9.5, and 4 kDa, consistent with the bands observed by SDS–PAGE. The five N-terminal amino acids of these fragments were sequenced, and this allowed an unambiguous assignment of the cleavage sites in the protein. The results show that the protein is cleaved at K57/R64 to generate the 25 and 4 kDa fragments. Cleavage of the 25 kDa fragment at R207 generates the 16 and 9.5 kDa fragments.

Two of the three residues are found in the active site. Both K57 and R64 reside in loop L1, where R64 forms part of the S1 binding pocket. R207 is in loop L3 and makes contacts in both the S1 and S3 binding sites. We consider the cleavages at K57 and R64 to be equivalent. Under these conditions, the cleavages at K57/R64 occur with a $t_{1/2}$ of <2 min, while the cleavage at R207 occurs with a $t_{1/2}$ of ~75 min. In the presence of an inhibitor (not shown), only R207 is protected from cleavage by trypsin.

One interpretation of the results shown in Figure 4A is that R207, on loop L3, is less accessible to trypsin than K57 and R64 on loop L1. However, it is possible that flanking residues and local structures may affect cleavage efficiency. Le Bonniec and co-workers (37) addressed this issue by examining the specificity of several proteases. They concluded that trypsin was the most efficient but least selective protease when compared to factor Xa and to thrombin. Of the five sites on the substrate (P3–P3′, excluding P1), the P1′ site exhibited the highest selectivity index for trypsin, although the value of 80 was significantly lower than that of thrombin (24 706). On the basis of the values published by Le Bonniec and co-workers, one can estimate that there is little difference in selectivity between the flanking sequences of K57 [FHK(57)STG], R64 [TSR(64)SGT], and R207 [SWR(207)NSK]. The predicted selectivity would differ by at most a factor of 3 between R207 and K57/R64. This difference is not sufficient to account for the factor of >40 in $t_{1/2}$. Thus, we suggest that the slower cleavage of R207 by trypsin demonstrates that the residue is less accessible than K57 and R64.

The limited trypsin digests of caspase-3 (Figure 4B) also show that both the large subunit (17 kDa) and the small subunit (12 kDa) are cleaved rapidly by the protease. In caspase-3, cleavage at K57/R64 in the large subunit gives a doublet at ~12 kDa and a band of 3.3 kDa (S29–K57). The small subunit is cleaved at R207, giving rise to 9.5 kDa (N208–H285) and 3.6 kDa (S176–R207) bands. Note that the 3.6 and 3.3 kDa bands are not visible in the gel shown in Figure 4B, although they are readily observed by MALDI-TOF mass spectrometry.

In the mature caspase-3, the cleavage at R207 was significantly faster ($t_{1/2} < 2$ min) when compared to that of procaspase-3 ($t_{1/2} \sim 75$ min), suggesting that the site becomes more accessible to the protease upon maturation of the procaspase. The rate of cleavage at K57/R64 remained fast in the mature caspase ($t_{1/2} < 2$ min). Experiments using less trypsin suggest that the cleavages occur ~10-fold faster in caspase-3 than in the procaspase (data not shown). As with the procaspase, R207 was protected in the presence of an inhibitor (data not shown). Overall, the data suggest that processing of the zymogen results in a more open active site conformation in the mature caspase that allows greater access to trypsin.

Limited Proteolysis with V8 Protease

We examined the conformation of procaspase-3(C163S) and of caspase-3 by limited V8 proteolysis, which cleaves at a position C-terminal to glutamate and aspartate residues. The time course analysis of V8 digestion of procaspase-3(C163S) at pH 7 is shown in Figure 5A and demonstrates four closely spaced bands between ~27 and 32 kDa. These fragments are termed bands 1–4, with band 1 being the full-length protein. These fragments were further cleaved into fragments of 16, 8.5, and 4 kDa.

As with the trypsin studies described above, we used MALDI-TOF mass spectrometry and N-terminal sequencing to unambiguously assign the cleavages to residues D9, E25, E98, E106, E173, D190, E248, and D253. The first cleavage occurs at E248 and D253, resulting in two fragments of ~29 and 4 kDa. The larger band is termed band 2, and band 2 is further cleaved at D9 and then at E25, both of which are in the pro domain, to give bands 3 and 4, respectively. Band 4 is then cleaved simultaneously at positions 98 and 106, and 173 and 190, giving rise to a mixture of ~16 and ~8.5 kDa bands.

The experiments were performed with procaspase-3(D$_3$A) (not shown), and we observed that, with the exception of cleavage at D9, the results were the same as those for procaspase-3(C163S). In addition, the presence of an inhibitor for both proteins did not result in significant protection of the cleavage sites (not shown).

For mature caspase-3, the results of limited V8 proteolysis are shown in Figure 5B. Overall, the same cleavages occur as for the procaspase, with the exceptions noted below. Importantly, no new cleavage sites appear upon zymogen processing. The results demonstrate three major bands (Figure 5B). The large subunit (17 kDa) is trimmed at the C-terminus, possibly at E173 (removing two residues), D169 (removing six residues), or E167 (removing eight residues). This produces a doublet consisting of the full-length and trimmed large subunits. The small subunit (12 kDa) is cleaved at E272, which removes the His tag at the C-terminus, producing a doublet consisting of two ~12 kDa fragments. The small subunit is cleaved further at E248/D253, resulting in an ~8 kDa fragment. The 4 kDa fragment is observed only in the overnight digests because cleavage at E272 results in two ~2 kDa fragments. Both of these fragments are observed by MALDI-TOF mass spectrometry. Interestingly, the cleavages at E98 and E106 and at D190 are not observed in caspase-3.

The results of the limited proteolysis studies (trypsin and V8) are shown in Figure 5C. The data are mapped onto the structure of mature caspase-3 to show the positions of the residues that are cleaved. As shown in this figure, E248 and D253 reside in loop L4, whereas E173 and D190 are in loops L2 and L2′, respectively. Residues E98 and E106 reside on the surface of the protein, away from the active site. In caspase-3 (10), E106 is observed to interact with R86, which resides on β-strand 2. This strand is the outside-most strand in the β-sheet, the edge of which is exposed to solvent. These results suggest that the salt bridge between R86 and E106 is not formed in the procaspase. Residue D190 is C-terminal to the blocking segment (K186–V189) described by Riedl *et al.* (20), so it is worth noting the

changes at this site. Residue D190 is not cleaved in caspase-3, suggesting that the exposed L2′ loop in procaspase-3 becomes less accessible for cleavage after zymogen processing. In caspase-3, D190 is within 3.3 Å of K137, on helix 3, whereas the distance between D190 and K137 in procaspase-7 is ~7.4 Å. Overall, the data are consistent with movements in loop L2′ upon maturation.

One of the advantages of V8 protease is that it is active over a broad pH range, with maximum activities around pH 4.0 and 7.8 (38). The activity varies only ~1.5-fold over this pH range. This allowed us to examine the cleavage of procaspase-3(C163S) and of caspase-3 between pH 8 and 4. These experiments were undertaken for two reasons. First, in the two structural studies (19, 20), the crystals were grown at pH 5.6 or 5.8. Second, Nicholson and co-workers (22) showed that the rate of autoactivation was pH-dependent, with a maximum rate obtained at pH ~5.5. In our experiments, the proteins were cleaved as described above for pH 7 (Figure 5), and the intensities of the bands were quantified at each time point. The data were then normalized relative to that of the full-length protein at time zero. Representative data for pH 7 are shown in Figure 5D for the seven major species, bands 1–4 and the 16, 8, and 4 kDa fragments. The data for bands 1–4 were fit to a double-exponential equation and for 16, 8, and 4 kDa fragments to a single-exponential equation to obtain k_{obs} values, the apparent rates of change for each species. These rates were then plotted versus pH, and the results are shown in Figure 5E. While this analysis allows us to summarize a large amount of data, we consider this to be a qualitative rather than a quantitative description of the results.

With respect to the four closely spaced bands (bands 1–4) of procaspase-3, the rates of the cleavages increased with a decrease in pH from 7 to 5. As shown in Figure 5E, the rates of disappearance of bands 1–4 increased ~20-fold from pH 7 to 5. This suggests greater accessibility to the protease at E248/D253, D9, and E25. We have shown that the pro domain of procaspase-3 binds to the protease domain at a site(s) away from the active site, although the binding site-(s) has not been identified (6). The data presented here suggest that the binding is pH-dependent. That is, the pro domain may be unbound and more solvent-exposed at lower pH, which allows faster cleavage by V8 protease. In addition, the data suggest a conformational change in loop L4 (E248/D253) at pH 5 that results in faster cleavage by the protease. As described below, this correlates with a change in the environments of the tryptophanyl residues in the active site.

Between pH 8 and 5, the cleavage of band 4 to generate the 16 and 8 kDa bands occurred at approximately the same rate. This suggests that the accessibility to V8 protease of the E98/E106 and E173/D190 sites does not change significantly over this pH range.

A second significant change occurred between pH 5 and 4, where at pH 4 the protein was more resistant to digestion. Over the time course of the experiment, we observed only band 1 and band 2, that is, cleavage at E248/D253. The data show that there was no cleavage in the pro domain (D9 or E25), nor were there cleavages at E98/E106 or E173/D190. The results suggest that with the exception of loop L4, the protein undergoes a conformational change between pH 5 and 4 that results in a protection of the remaining sites of proteolysis.

In comparison with procaspase-3(C163S), the mature caspase-3 was cleaved faster at the E248/D253 sites at pH 4 than at higher pH values (data not shown). For example, cleavage at E248/D253 occurred with $t_{1/2}$ of ~3 h at pH 4 versus a $t_{1/2}$ of >8 h at pH 7, so at pH 4 the 12 kDa small subunit disappeared in the overnight samples. This can be compared to the data in Figure 5B, which show that the small subunit persists after overnight digestion. In contrast to the data at pH 7, there was less cleavage at E272, which eliminated the ~12 kDa doublet and resulted in the appearance of the 4 kDa fragment at the early time points.

Overall, the data show that for both the procaspase and the mature caspase, cleavage at E248/D253 occurs faster at lower pH values than at pH 7. This is consistent with a pH-dependent conformational change in loop L4.

Fluorescence Quenching

Each monomer of the procaspase-3 dimer contains two tryptophanyl residues, W206 and W214, both of which are in the active site. According to the structures of procaspase-7, W206, in loop L3, is completely solvent exposed (see Figure 1). Upon maturation, loop L3 moves into the active site such that W206 stacks onto W214, a movement of ~10 Å.

We examined the fluorescence emission of two mutants of procaspase-3 in which the tryptophans were replaced to generate W206Y or W214V. Both mutants were in the context of an active site mutation, C163A. The results are shown in Figure 6A. Overall, there was a decrease in fluorescence emission for both mutants, but surprisingly, the fluorescence emissions were blue-shifted compared to that of procaspase-3(C163S). The wavelength maxima for caspase-3, procaspase-3(C163S), procaspase-3(C163A/W206Y), and procaspase-3(C163A/W214V) are 342, 340, 337, and 335 nm, respectively. The results are unexpected because the structure of procaspase-7 predicts that procaspase-3(C163A/W214V) would have a red-shifted fluorescence emission compared to the wild-type procaspase if loop L3, containing W206, were unraveled and solvent-exposed.

We examined the fluorescence emission of procaspase-3(C163S) and of procaspase-3(D_3A) in the presence or absence of an inhibitor, and the results are shown in panels B and C of Figure 6. The proteins were excited at 280 nm, to excite all aromatic residues (Figure 6B), or at 295 nm, to excite the tryptophans only (Figure 6C). The results show that there was no difference in the fluorescence emission upon inhibitor binding. If binding of an inhibitor induced W206, on loop L3, to move 10 Å to stack on W214, then the movement should be reflected by a change in the fluorescence emission. The results of panels B and C of Figure 6 suggest that the environments of the tryptophans change little upon inhibitor binding. For procaspase-3(D_3A), we measured the enzymatic activity before and after addition of an inhibitor. The results are shown in Figure 6D and demonstrate the loss of activity upon inhibitor binding. While there is no change in fluorescence emission (Figure 6B,C), the data show that the inhibitor is bound to the protein. In Figure 4, we noted the protection of R207 from trypsin proteolysis in the presence of inhibitor. The results suggested either that loop 3 was inserted into the active site before inhibitor binding, and hence R207 was protected, or that the binding of an inhibitor facilitated the correct conformation of loop L3. The results shown in panels B–D of Figure 6 suggest that the binding of an inhibitor does not facilitate movement of loop L3, but rather the loop is inserted into the active site in the apoprocaspase.

Because of these results, we examined the accessibility of the tryptophans to quenching by potassium iodide, and the experiments were performed over the pH range of 9–3. Representative data for procaspase-3(C163S) are shown in Figure 6E. The data at each pH were fit to eq 2, as described in Materials and Methods, to determine the Stern–Volmer quenching constant, K_{SV}. The constants were plotted versus pH, and the results are shown in Figure 6F for the four proteins. For all proteins at pH >8, values for K_{SV} are ~3–8. Both caspase-3 and procaspase-3 demonstrate two transitions, although one transition results in the opposite effect for the proteins. For example, between pH 9 and 6, K_{SV} increases to ~13 for procaspase-3, whereas it decreases from ~8 to ~6 for caspase-3. Although the transition is small for caspase-3, it is reproducible. The transition results in an increased accessibility to iodide in the case of procaspase-3 and a decrease in iodide accessibility for the mature caspase-3. In contrast to these two proteins, the two tryptophan mutants demonstrate a single

transition (Figure 6F). All four proteins show a cooperative increase in K_{SV} between pH 6 and 3, with the final values between ~18 and 25.

The data shown in Figure 6F were fit to eq 3, as described in Materials and Methods, to determine the apparent pK values for the transitions. In the case of the tryptophan mutants, a modified form of eq 3 was used to account for the single transition. For the first transition, the pK_a values for procaspase-3(C163S) and mature caspase-3 were 4.1 ± 0.3 and 4.0 ± 0.2, respectively. The pK_a values for procaspase-3(C163A/W206Y) and procaspase-3(C163S/W214V) were 4.8 ± 0.1 and 4.7 ± 0.03, respectively. These results are consistent with the titration of one or more acidic groups that affect the environment of the tryptophanyl residues in the active sites. It is not clear why the pK_a values are higher for the tryptophanyl mutants or why these proteins demonstrate a single transition, but the data suggest that removal of one tryptophan changes the environment of the second tryptophan. The second transition for mature caspase-3 has a pK_a of 7.2 ± 0.4, whereas that for procaspase-3 is 7.7 ± 0.4. The second transition is consistent with the titration of a histidyl residue, which again affects the environment of the tryptophanyl residues in the active sites.

The results also are consistent with an increased level of solvent exposure of the tryptophanyl side chains as the pH is lowered. To examine this, we used acrylamide and cesium chloride as quenching agents. The results for acrylamide quenching, at pH 7, are shown in Figure 6G. The data demonstrate that there is little quenching of the fluorescence emission by this quenching agent. Moreover, there are no differences among the four proteins. For comparison, procaspase-3(C163S) was unfolded in buffer containing 8 M urea, and the data demonstrate an increase in the Stern–Volmer quenching constant for the unfolded protein due to the exposure of the tryptophanyl side chains. These results would be expected for native procaspase-3(C163A/W214V) if W206 were solvent-exposed in the native protein. As with potassium iodide, the experiments with acrylamide were performed over the pH range of 7–3, and the results are shown in Figure 6F (bottom panel). The data demonstrate that there was no change in K_{SV} for acrylamide over this pH range. In addition, we repeated the experiments using cesium chloride as the quenching agent, and the results were the same as for acrylamide (Figure 6F, bottom panel). There was no change in K_{SV} from pH 7 to 3. These results suggest that the conformational change that occurs between pH 6 and 4 likely affects the microenvironment of the tryptophanyl residues so that the tryptophans are more accessible to quenching by iodide. That is, at lower pH, the negative charge(s) around the tryptophans decreases, resulting in an increased level of quenching by the negatively charged iodide ion. Overall, the results demonstrate that the tryptophans are not exposed to solvent, even at the lower pH. This interpretation is consistent with the results of the limited trypsin proteolysis, presented above, in which it was shown that at pH 7.2 R207, in loop L3, is cleaved more slowly than R64, in loop L1, and is protected upon substrate binding.

Tryptophan Fluorescence as a Function of pH

Fluorescence emission scans of procaspase-3(C163S) and of mature caspase-3 were examined over the pH range of 2.5–9, and the average emission wavelength was calculated at each pH using eq 4, as described in Materials and Methods. The results of the calculations are shown in Figure 7. In the case of procaspase-3(C163S), the average emission wavelength, $\langle\lambda\rangle$, is constant at 343 nm between pH 5.5 and 9.0. Below pH 5.5, there is a cooperative decrease in $\langle\lambda\rangle$ such that at pH <3.5, $\langle\lambda\rangle$ is 341 nm. This represents a blue shift in the fluorescence emission as the pH is lowered. In addition, there is a small inflection at pH 4 ($\langle\lambda\rangle$ = 341.4 nm). The data for procaspase-3(C163S) were fit to eq 5, as described in Materials and Methods, and the following pK_a values were determined for the two transitions: pK_{a1} = 3.7 ± 0.1 and pK_{a2} = 4.7 ± 0.1.

In contrast, the results for the mature caspase-3 are very different. The average emission wavelength for caspase-3 reached a maximum between pH 7.0 and 9.0, where $\langle\lambda\rangle = 344.6$ nm. Below pH 7, there was a cooperative decrease in $\langle\lambda\rangle$ to 341.2 nm at pH 4. Below pH 4, a second cooperative transition occurred that resulted in an increase in $\langle\lambda\rangle$, representing a red shift in the fluorescence emission so that $\langle\lambda\rangle = 342.5$ nm. The data were fit to eq 5, and the following apparent pK_a values were determined: $pK_{a1} = 3.0 \pm 0.2$ and $pK_{a2} = 5.7 \pm 0.1$. For both proteins, the results shown in Figure 7 were identical regardless of whether the proteins were titrated from pH 9 to 2.5 or from pH 2.5 to 9, demonstrating the reversibility of the transitions (Figure 7).

A comparison of the data in Figure 7 shows that the proteins differ in four aspects. First, at pH >7, the fluorescence emission is red-shifted upon maturation of the caspase. This is consistent with a more solvent accessible active site as shown by the proteolysis studies. This also agrees with the enzyme activity measurements, which suggest that the active site loops adopt a more open conformation upon processing, resulting in a decrease in the pK_a values of the two catalytic groups. Second, the major transitions between pH ~6 and 4 have different pK_a values. The data are consistent with the protonation of an acidic group, and this process affects the environment of the tryptophanyl residues. If we assume that the same group is titrated in the two proteins, then the data suggest that the environment of the acidic group is not equivalent in the two forms of the protein. Alternatively, the results for caspase-3 are consistent with the titration of a histidyl side chain. Third, below pH 4, a smaller transition occurs in procaspase-3, and this transition results in a small blue shift in fluorescence emission. Fourth, an additional transition occurs in the mature caspase-3 below pH 4, and this transition results in a red shift in fluorescence emission. This transition may be due to acidic groups at the C-terminus of the large subunit in the mature caspase. In the procaspase, these residues are sequestered in the inter-subunit linker.

While the precise groups that are responsible for the transitions are not known, the protonation and/or deprotonation of the groups affects the environment of the tryptophanyl residues in the active site. Protonation of the acidic group may be responsible for the increase in K_{SV} for iodide quenching (Figure 6C) and may explain why there is no increase in K_{SV} for cesium or acrylamide at lower pH. Overall, the data suggest that one or more salt bridges affect the stability of the active site.

DISCUSSION

One underlying question in the studies of caspases is why the procaspases are not active in the cell. It is thought that the upstream caspases are stored as inactive monomers until apoptotic signals facilitate their dimerization and subsequent autoactivation. Less clear is why the downstream, executioner procaspases are inactive because they are known to be homodimers in the cell (8). The recent structures of procaspase-7 (19, 20) suggest mechanisms for the procaspase dormancy. The C-terminal region of the intersubunit linker, called the blocking segment (K186–V189), occupies the central cavity and prevents insertion of the elbow loop region of loop L3 from the opposite monomer. As a consequence, loop L3 is unraveled and solvent-exposed. In addition, the covalent connectivity between the subunits prevents formation of the loop bundle among loops L4, L2, and L2′. Thus, the contacts that stabilize these loops in the active caspase have not formed in the procaspase. Upon cleavage at D175, loops L3 and L4 move to positions similar to those found in the active caspase, but loop L2′ remains in the closed conformation, that is, bound in the central cavity. Once the substrate or inhibitor binds, loop L2′ flips 180° to contact loops L2 and L4, forming the loop bundle. Overall, the procaspase-7 structures show that the incomplete formation of the S1, S2, and S4 subsites is incompatible with the binding of peptide substrates.

Nicholson and co-workers showed that procaspase-3 is catalytically competent (22), although the steady-state parameters were not described. Using a triple mutant in which the three processing sites were removed (D9A/D28A/D175A), we show here that the activity of procaspase-3 is ~200-fold lower than that of the mature caspase-3. Other uncleavable procaspases have been described as catalytically competent as well (22). Here, we show that procaspase-3(D_3A) binds substrate efficiently, but catalysis is much slower than for the mature caspase. In addition, we show that the pK_a values of the active site H121 and C163 are higher by ~1 pH unit than that of the mature caspase-3. It has been shown that during apoptosis, the pH of the cell decreases from 7.4 to ~6.8 (39). Over this pH range, the activity of caspase-3 is nearly optimal, whereas that of procaspase-3 represents only ~20% of the maximal activity observed at pH 8.2.

While it is possible that the procaspase-3(D_3A) is processed at alternate sites, and in concentrations below the detection limits of the experiments described here, to generate a "superactive" caspase-3, it seems unlikely on the basis of our experimental results. A reasonable conclusion from our results is that the procaspase-3 is catalytically competent. The protein binds peptide substrates efficiently, like the mature caspase-3, but the catalytic efficiency is ~130-fold lower than that of the mature caspase-3. The pH profile suggests that the environments of both H121 and C163 are altered in the procaspase compared to their environments in the mature caspase, resulting in an increase in the pK_a values by ~1 pH unit.

The data suggest a structural model in which loop L3 is inserted into the active site, with consequential formation of the substrate binding pocket. We note here that experiments performed on the triple mutant are only suggestive of the wild-type protein since point mutations may have effects on local secondary structures. However, we also note that with the exception of the activity measurements, procaspase-3(D_3A) and procaspase-3(C163S) are interchangeable in the biochemical and biophysical studies described here. The inactive procaspase-3(C163S), which is similar to the C163A mutant used in the structural studies (19, 20), contains the three processing sites. Our results indicate that replacing the three aspartates with alanine has minimal effects on the protein structure, but the conclusions are tempered by our work on a mutant rather than the wild-type protein.

Our suggestion of a structural model in which loop L3 is inserted into the active site, with consequential formation of the substrate binding pocket, is supported by the following observations. First, trypsin cleaves R207, in loop L3, much more slowly than K57/R64, in loop L1, with a difference in $t_{1/2}$ values of a factor of >40 (<2 vs ~75 min). In addition, R207 is protected from cleavage upon binding of an inhibitor. Second, fluorescence emission studies showed that W206, on loop L3, is not solvent-exposed but rather appears to be close to W214 in the active site. This was shown by a blue shift in the fluorescence emission wavelength maximum of the two tryptophan mutants, W206Y and W214V. If W206 were exposed to solvent in the procaspase, then one would expect a red-shifted fluorescence emission in the W214V mutant. In addition, there was no change in the tryptophan fluorescence emission of the procaspase upon binding of an inhibitor, again suggesting that W206 is close to W214 in the procaspase. Third, fluorescence emission and quenching studies showed that, at pH >7, the tryptophans are less solvent accessible in the procaspase than in the mature caspase. This is observed as a red shift in the tryptophan fluorescence emission upon maturation, consistent with an opening of the active site. A more open active site is shown also by the increase in the accessibility of R207 to cleavage by trypsin in the mature caspase. This is consistent with a decrease in the pK_a values of the two catalytic groups upon maturation. The accessibility of the negatively charged iodide quencher was low at pH >7 and increased at lower pH, with two transitions observed. While it is not yet clear what these titrations represent in terms of conformational changes in the protein, the protonations leading to the conformational change appear to affect the

electrostatic environment of the tryptophanyl residues by making it more electropositive rather than facilitating the unraveling of loop L3. This is supported by the observations that there was no effect of pH on the accessibility of either acrylamide or cesium in the fluorescence quenching studies. It is worthwhile to note that the fluorescence emission and quenching results obtained at the lower end of the pH range (pH 2.4–4) had no significant impact with respect to the two main conclusions reached in this study: that the unprocessed procaspase-3 mutant retains some enzymatic activity and that it probably possesses some structural features in the active site resembling those in mature caspase-3. However, the broader pH range allows the calculation of the pK_a values, even though at this point the responsible groups are unknown. We showed that the transitions are reversible (Figure 7), and our protein folding results at pH 4 (K. Bose and A. C. Clark, unpublished results) demonstrate that the protein folds reversibly under these conditions. We suggest that the conformational changes described here do not result in complete solvent exposure of the tryptophans, as would be observed in the unfolded protein. This interpretation is consistent with the blue-shifted fluorescence emission observed at lower pH (below pH ~5).

The presence of a well-formed active site has been observed in the zymogens of other proteases, although the precise mechanisms of their activation differ (40). In lysosomal cathepsins, the active site is fully formed, but the pro domain interacts with the active site and prevents maturation (41). The activation is triggered by a drop in pH that substantially weakens the interaction between the propeptide and the catalytic domain, resulting in widening the active site cleft (42). In the trypsin family of serine proteases, the dislocated catalytic machinery of trypsinogen undergoes reorientation after proteolysis at R15 (42). Here, we suggest that the procaspase-3 dimer has an intact substrate binding pocket, like caspase-3, and the active site in caspase-3 adopts an open conformation after cleavage of the intersubunit linker. Cleavage at D175 allows the linker to move away from the catalytic groove and form the loop bundle.

We suggest that formation of the loop bundle is critical in opening and stabilizing the active site. The contacts formed among loops L2, L4, and L2′ may move loop L4 away from the catalytic groove, further opening the active site. Loop L4 has four phenylalanine residues in the proximity of the tryptophans. Positioning the phenylalanines close to the tryptophans could account for the blue-shifted fluorescence emission observed for the procaspase. Upon maturation, conformational changes in loops L4 and L2 may open the active site, consistent with the structural studies. These movements allow the C163 side chain to rotate toward the S1 subsite and hence form the oxyanion hole.

This mechanism stresses the importance of dimerization on active site formation. Indeed, it is generally accepted that caspase monomers are inactive. The best evidence for this is observed in caspase-9 (43), although it also has been shown in caspase-1 (44). Under normal physiological conditions, caspase-9 is a monomer, and activity is associated with the formation of transient dimers (43). In the absence of the dimeric structure, the loop bundle cannot form.

It is worth noting that the recognition sequence in the intersubunit linker of the executioner (caspase-3) subfamily is not optimized for autoactivation. The caspases in this subfamily prefer the sequence DEXD (45), whereas the sequence in the intersubunit linker is IXXD. The (I/V/L)-EXD sequence is preferred by caspase-6, -8, -9, and –10 (45). In contrast, procaspases in the caspase-1 subfamily are activated following cleavage at WXXD in the intersubunit linker. The WEXD sequence is preferred by the caspase-1 subfamily (45) and is in keeping with the general idea of a scaffold-mediated autoactivation. This may add another level of control to attenuation of the autoactivation of the executioner procaspases.

Acknowledgments

References

1. Earnshaw WC, Martins LM, Kaufmann SH. Annu Rev Biochem. 1999; 68:383–424. [PubMed: 10872455]

2. Stennicke HR, Salvesen GS. Biochim Biophys Acta. 1998; 1387:17–31. [PubMed: 9748481]

3. Kumar S. Clin Exp Pharmacol Physiol. 1999; 26:295–303. [PubMed: 10225139]

4. Garcia-Calvo M, Peterson EP, Villiancourt JP, Zamboni R, Nicholson DW, Thornberry NA. Cell Death Differ. 1999; 6:362–369. [PubMed: 10381624]

5. Thornberry NA, Rano TA, Peterson EP, Rasper DM, Timkey T, Carcia-Calvo M, Hotzager VM, Nordstrom PA, Roy S, Vaillancourt JP, Chapman KT, Nicholson DW. J Biol Chem. 1997; 272:17907–17911. [PubMed: 9218414]

6. Pop C, Chen YR, Smith B, Bose K, Bobay B, Tripathy A, Franzen S, Clark AC. Biochemistry. 2001; 40:14224–14235. [PubMed: 11714276]

7. Bose K, Clark AC. Biochemistry. 2001; 40:14236–14242. [PubMed: 11714277]

8. Cohen G. Biochem J. 1997; 326:1–16. [PubMed: 9337844]

9. Saunders PA, Cooper JA, Roodell MM, Schroeder DA, Borchert CJ, Isaacson AL, Schendel MJ, Godfrey KG, Cahill DR, Walz AM, Loegering RT, Gaylor H, Woyno IJ, Kaluyzhny AE, Krzyzek RA, Mortari F, Tsang M, Roff CF. Anal Biochem. 2000; 284:114–124. [PubMed: 10933864]

10. Mittl PRE, DiMarco S, Krebs JF, Bai X, Karanewsky DS, Priestle JP, Tomaselli KJ, Grutter MG. J Biol Chem. 1997; 272:6539–6547. [PubMed: 9045680]

11. Rotonda J, Nicholson DW, Fazil KM, Gallant M, Gareau Y, Labelle M, Peterson EP, Rasper DM, Ruel R, Vaillancourt JP, Thornberry NA, Becker JW. Nat Struct Biol. 1996; 3:619–625. [PubMed: 8673606]

12. Walker NPC, Talanian RV, Brady KD, Dang LC, Bump NJ, Ferenz CR, Franklin S, Ghayur T, Hackett MC, Hammill LD, Herzog L, Hugunin M, Houy W, Mankovich JA, McGuiness L, Orlewicz E, Paskind M, Pratt CA, Reis P, Summani A, Terranova M, Welch JP, Xiong L, Moller A, Tracey DE, Kamen R, Wong WW. Cell. 1994; 78:343–352. [PubMed: 8044845]

13. Wilson KP, Black JAF, Thomson JA, Kim EE, Griffith JP, Navia MA, Murcko MA, Chambers SP, Aldape RA, Raybuck SA, Livingston DJ. Nature. 1994; 370:270–275. [PubMed: 8035875]

14. Watt W, Koeplinger KA, Mildner AM, Heinrikson RL, Tomasselli AG, Watenpaugh KD. Structure. 1999; 7:1135–1143. [PubMed: 10508785]

15. Wei Y, Fox T, Chambers SP, Sintchak J, Coll JT, Golec JMC, Swenson L, Wilson KP, Charifson PS. Chem Biol. 2000; 7:423–432. [PubMed: 10873833]

16. Chai J, Shiozaki E, Srinivasula SM, Wu Q, Dataa P, Alnemri ES, Shi Y. Cell. 2001; 104:769–780. [PubMed: 11257230]

17. Han Z, Hendrickson EA, Bremner TA, Wyche JH. J Biol Chem. 1997; 272:13432–13436. [PubMed: 9148968]

18. Stennicke HR, Jurgensmeier JM, Shin H, Deveraux Q, Wolf BB, Yang X, Zhou Q, Ellerby M, Ellerby LM, Bredesen D, Green DR, Reed JC, Froelich CJ, Salvesen GS. J Biol Chem. 1998; 273:27084–27090. [PubMed: 9765224]

19. Chai J, Wu Q, Shiozaki E, Srinivasula SM, Alnemri ES, Shi Y. Cell. 2001; 107:399–407. [PubMed: 11701129]

20. Riedl SJ, Fuentes-Prior P, Renatus M, Kairies N, Krapp S, Huber R, Salvesen GS, Bode W. Proc Natl Acad Sci USA. 2001; 98:14790–14795. [PubMed: 11752425]

21. Shi Y. Mol Cell. 2002; 9:459–470. [PubMed: 11931755]

22. Roy S, Bayly CI, Gareau Y, Houtzager VM, Kargman S, Keen SLC, Rowland K, Seiden IM, Thornberry NA, Nicholson DW. Proc Natl Acad Sci USA. 2001; 98:6132–6137. [PubMed: 11353841]

23. Gu Y, Wu J, Faucheu C, Lalanne JL, Diu A, Livingston DJ, Su MSS. EMBO J. 1995; 14:1923–1931. [PubMed: 7743999]

24. Muzio M, Stockwell BR, Stennicke H, Salvesen GS, Dixit VM. J Biol Chem. 1998; 273:2926–2930. [PubMed: 9446604]

25. Stennicke HR, Deveraux QL, Humke EW, Reed JC, Dixit VM, Salvesen GS. J Biol Chem. 1999; 274:8359–8362. [PubMed: 10085063]

26. Edelhoch H. Biochemistry. 1967; 6:1948–1954. [PubMed: 6049437]

27. Stennicke HR, Salvesen GS. Methods. 1999; 17:313–319. [PubMed: 10196102]

28. Stennicke HR, Salvesen GS. J Biol Chem. 1997; 272:25719–25723. [PubMed: 9325297]

29. Tang SS, Chang GG. Biochem J. 1996; 315:599–606. [PubMed: 8615835]

30. Tobin H, Staehelin T, Gordon J. Proc Natl Acad Sci USA. 1979; 76:4350–4354. [PubMed: 388439]

31. Lakowicz, JR. Principles of fluorescence spectroscopy. Plenum Press; New York: 1983.

32. Royer CA, Mann CJ, Matthews CR. Protein Sci. 1993; 2:1844–1852. [PubMed: 8268795]

33. Bhuyan AK, Udgaonkar JB. J Mol Biol. 2001; 312:1135–1160. [PubMed: 11580255]

34. Stennicke HR, Renatus M, Meldal M, Salvesen GS. Biochem J. 2000; 350:563–568. [PubMed: 10947972]

35. Talanian RV, Quinlan C, Trautz S, Hackett MC, Mankovich JA, Banach D, Ghayur T, Brady KD, Wong WW. J Biol Chem. 1997; 272:9677–9682. [PubMed: 9092497]

36. Lewis SD, Johnson FA, Shafer JA. Biochemistry. 1981; 20:48–51. [PubMed: 7470479]

37. Bianchini EP, Louvain VB, Marque PE, Juliano MA, Juliano L, Le Bonniec BF. J Biol Chem. 2002; 277:20527–20534. [PubMed: 11925440]

38. Drapeau G, Boily Y, Houmard J. J Biol Chem. 1972; 247:6720–6726. [PubMed: 4627743]

39. Gottlieb RA, Nordberg J, Skowronski E, Babior BM. Proc Natl Acad Sci USA. 1996; 93:654–658. [PubMed: 8570610]

40. Turk B, Turk D, Turk V. Biochim Biophys Acta. 2000; 1477:98–111. [PubMed: 10708852]

41. Rozman J, Stojan J, Kuhelj R, Turk V, Turk B. FEBS Lett. 1999; 459:358–362. [PubMed: 10526165]

42. Zhuang P, Butterfield D. Biotechnol Prog. 1992; 8:204–210. [PubMed: 1369378]

43. Renatus M, Stennicke HR, Scott FL, Liddington RC, Salvesen GS. Proc Natl Acad Sci USA. 2001; 98:14250–14255. [PubMed: 11734640]

44. Van Criekinge W, Beyaert R, Van de Craen M, Vandenabeele P, Schotte P, De Valck D, Fiers W. J Biol Chem. 1996; 271:27245–27248. [PubMed: 8910297]

45. Grutter M. Curr Opin Struct Biol. 2000; 10:649–655. [PubMed: 11114501]

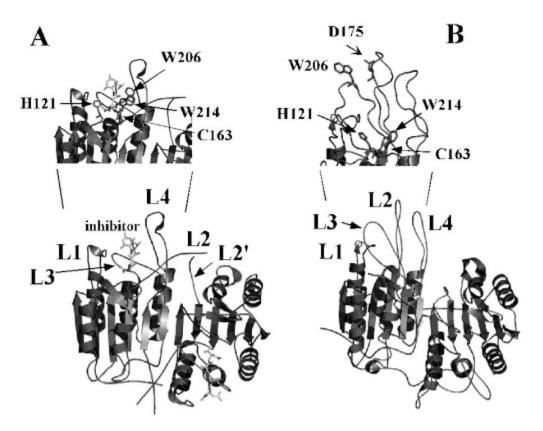46. Pop C, Feeney B, Tripathy A, Clark AC. Biochemistry. 2003; 42:12311–12320. BI034998X. [PubMed: 14567692]

Figure 1.
Mature caspase-3 (inhibitor bound) structure (PDB entry 1CP3) (A) and procaspase-7 structure (PDB entry 1GQF) (B) generated with *PyMOL* (Delano Scientific). For panels A and B, L1 (residues 52–64), L2 (residues 163–175), L2′ (residues 176′–192′), L3 (residues 198–213), and L4 (residues 246–263) represent the five active site loops as described in the text. The prime indicates residues from the second heterodimer. The two tryptophan residues (W206 and W214), the cleavage site aspartate residue (D175), and the two catalytic residues (H121 and C163) are highlighted in the inset (caspase-3 numbering). For clarity, only one active site is labeled for the two proteins.
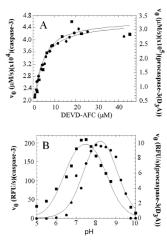
Figure 2.
(A) Plot of initial velocity (v_0) vs substrate concentration for procaspase-3(D_3A) (●) and mature caspase-3 (■) at pH 7.5. Concentrations of procaspase-3(D_3A) and mature caspase-3 were 10 and 1 nM, respectively. (B) Effect of pH on initial velocity (v_0) for procaspase-3(D_3A) (●) and mature caspase-3 (■). The solid lines represent fits to the Michaelis–Menten equation for panel A and to eq 1 for panel B as described in Materials and Methods. The parameters for the fits for panels A and B are shown in Table 1.
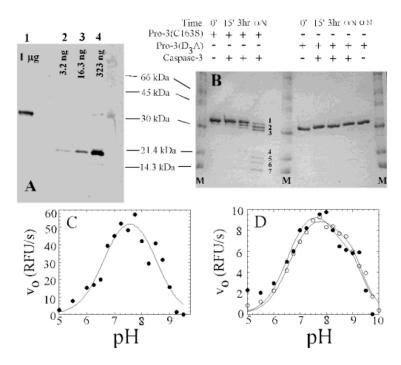
Figure 3.
Characterization of procaspase-3(D$_3$A). (A) Anti-caspase-3 immunoblot of procaspase-3(D$_3$A) (lane 1) and of mature caspase-3 (lanes 2–4). Protein concentrations are indicated above each lane, and sizes of molecular mass markers are indicated. (B) Procaspase-3(C163S) or procaspase-3(D$_3$A) incubated with mature caspase-3. M refers to molecular mass markers. The lines indicate the sizes of each marker. Bands 1–7 are described in the text. (C) Activity (v_0) of mature caspase-3 (50 pM) vs pH. The solid line represents a fit of the data to eq 1 as described in Materials and Methods. The parameters obtained rom the fits are as follows: pK_{a1} = 6.6 and pK_{a2} = 8.5. The optimal pH range was 7.2–7.8. (D) Activity (v_0) of a mixture of procaspase-3(D$_3$A) (10 nM) and mature caspase-3 (50 pM) vs pH (●). The two individual experiments from Figure 2B were scaled and added and are shown for comparison (○). The solid lines represent fits to a modified form of eq 1 representing two independent enzyme activities.
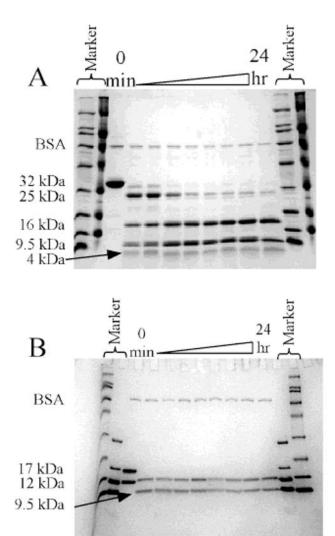
Figure 4.
(A) Trypsin digestion of procaspase-3(C163S) at pH 7.2. The 32 kDa band represents the full-length procaspase-3(C163S), whereas the 25, 16, 9.5, and 4 kDa bands are the cleavage products as described in the text. (B) Trypsin digestion of mature caspase-3 at pH 7.2. The 17 and 12 kDa bands represent the large and small subunits, respectively. The 9.5 kDa band represents the cleavage product as described in the text. A known amount of BSA was added for normalization.
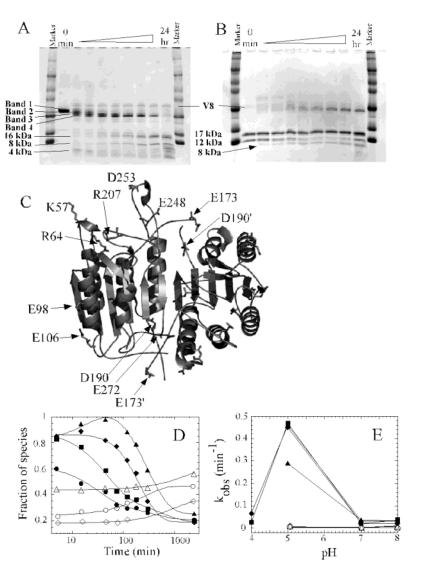
Figure 5.
(A) V8 protease (Endo-Glu C) digests of procaspase-3(C163S) at pH 7.0. (B) V8 protease digests of mature caspase-3 at pH 7.0. (C) Trypsin and V8 protease cleavage sites of procaspase-3(C163S) are mapped onto the caspase-3 structure. The structure was generated using the program *PyMOL* (Delano Scientific). The cleavages at K57, R64, and R207 are by trypsin, and the cleavages at E98, E106, E173, D190, E248, D253, and E272 are by V8 protease. The prime indicates residues from the second heterodimer. Note that the inhibitor has been removed and only half of the protein is labeled for clarity. (D) Fraction of species vs time for procaspase-3(C163S) at pH 7.0. (E) Plot of k_{obs} vs pH for the procaspase-3(C163S) fragments. In panels D and E, the bands are shown as follows: band 1 (●), band 2 (■), band 3 (◆), band 4 (▲), 16 kDa band (○), 8 kDa band (◇), and 4 kDa band (△). Solid lines in panel D represent fits of the data as described in Materials and Methods. Bands 1–4 were fit to a double-exponential equation, while the 16, 8, and 4 kDa bands were fit to a single-exponential equation. The rates of disappearance (k_{obs}) of bands 1–4 and the rates of formation (k_{obs}) of the 16, 8, and 4 kDa bands from the fits were plotted vs pH as shown in panel E. The points in panel E were joined by solid lines.
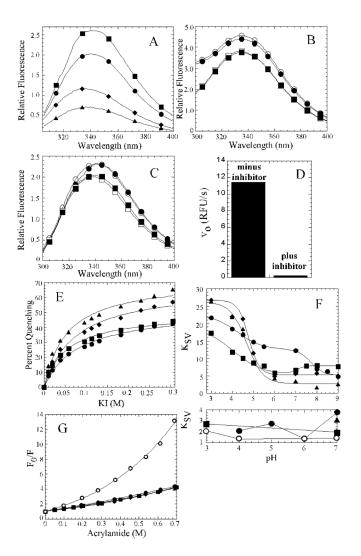
Figure 6.
(A) Fluorescence emission scans of procaspase-3(C163S) (●), mature caspase-3 (■), procaspase-3(C163A/W206Y) (▲), and procaspase-3(C163A/W214V) (◆). Samples were excited at 295 nm, and emission was monitored between 305 and 400 nm. (B and C) Fluorescence emission scans of procaspase-3(C163S) (○ and ●) or procaspase-3(D$_3$A) (□ and ■) in the absence (empty symbols) or presence (filled symbols) of the inhibitor (Z-VAD-FMK). Samples were excited at 280 (B) or 295 nm (C). (D) Activity (v_0) of procaspase-3(D$_3$A) before or after inhibition with Z-VAD-FMK. Procaspase-3(D$_3$A) (0.5 μM) was incubated with Z-VAD-FMK (5 μM) in assay buffer (pH 7.8), and the enzymatic activity was determined as described in Materials and Methods. (E) Plot of percent quenching by iodide vs pH for procaspase-3(C163S) at pH 7.0 (●), 6.0 (■), 5.0 (◆), and 4.0 (▲). (F) In top panel are shown Stern–Volmer quenching constants (K_{SV}) for quenching by iodide vs pH for procaspase-3(C163S) (●), procaspase-3(C163A/W206Y) (▲), procaspase-3(C163A/W214V) (◆), and mature caspase-3 (■). In the bottom panel are shown Stern–Volmer quenching constants (K_{SV}) for quenching by acrylamide vs pH for procaspase-3(C163S) (●), procaspase-3(C163A/W206Y) (▲), and mature caspase-3 (■) and Stern–Volmer quenching constants (K_{SV}) for quenching by CsCl vs pH for procaspase-3(C163S) (○). (G) Acrylamide quenching of procaspase-3(C163S) (●), procaspase-3(C163A/W206Y) (▲), procaspase-3(C163A/W214V) (◆), mature caspase-3

(■), and procaspase-3(C163S) in buffer containing 8 M urea (○) at pH 7. Data were fit to eqs 2 and 3 for panels E and F (top panel), respectively. For panel G, the data were fit to the Stern–Volmer equation that accounts for dynamic and static quenching as described in the text.
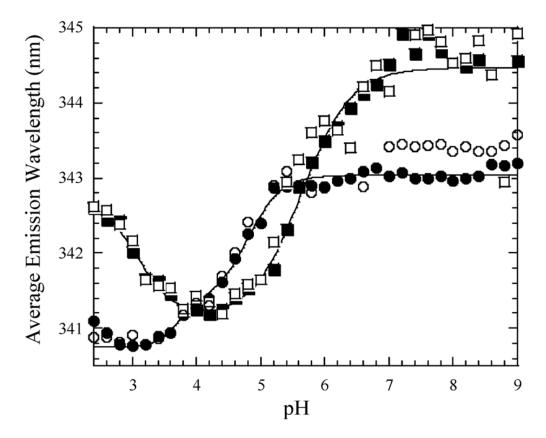
Figure 7.
Average emission wavelength ($\langle \lambda \rangle$) vs pH for procaspase-3(C163S) (● and ○) and mature caspase-3 (■ and □). Filled symbols represent titrations from pH 9 to 2.4, and empty symbols represent titrations from pH 2.4 to 9. Solid lines represent fits of the data to eq 5 as described in Materials and Methods. The parameters obtained from the fits are described in the text.

Table 1

Catalytic Parameters for Caspase-3 and Procaspase-3(D$_3$A)

	caspase-3	procaspase-3(D$_3$A)
K_m (μM)	2.2 ± 0.5	3.5 ± 0.8
k_{cat} (s^{-1})	0.4 ± 0.05	$(1.4 ± 0.003) \times 10^{-4}$
k_{cat}/K_m (M^{-1} s^{-1})	1.8×10^5	8.6×10^2
optimal pH	7.2–7.8	8.0–8.5
pK_{a1}	6.3	7.3
pK_{a2}	8.5	9.1